VIP Imaging Agents

DOI: 10.1002/ange.201000075

# Bimodal MR–PET Agent for Quantitative pH Imaging**

*Luca Frullano, Ciprian Catana, Thomas Benner, A. Dean Sherry, and Peter Caravan**

The scope of magnetic resonance imaging (MRI) is moving beyond anatomical and functional imaging to also convey information at the molecular level. Molecular MRI is enabled by the introduction of protein-targeted contrast agents[1] as well as "smart" or activatable contrast agents.[2] MR contrast agents induce relaxation of tissue water, and the extent of this relaxation enhancement, termed relaxivity ($r_1$), depends on a number of molecular factors, including the hydration state of the contrast agent and its rotational diffusion rate. In a seminal study, Meade and co-workers demonstrated that the relaxivity of a specifically designed contrast agent could be changed in the presence of the enzyme β-galactosidase and thus created an imaging agent whose signal was activated by the presence of the enzyme.[3,4] Numerous publications have followed in the last decade that describe "smart" agents that are responsive to other enzymes, to changes in the pH, to the concentration of specific metal ions, to partial oxygen pressure, or to temperature.[5,6]

The impressive gains in the development of smart agents have been slow to have an impact on in vivo imaging studies, however, as can be appreciated from Equation (1), which relates the rate of water relaxation, $1/T_1$, to $r_1$. The MR signal is a function of $T_1$ [Eq. (1); $\frac{1}{T_1^0}$ is the relaxation rate in the absence of an agent], which depends on both $r_1$ and the contrast-agent concentration, [Gd]. In vitro, the gadolinium concentration is known and fixed; any signal change is due to a change in relaxivity. In vivo, the agent concentration is unknown, will change with time, and may vary in diseased versus normal tissue.

$$\frac{1}{T_1} = r_1[\mathrm{Gd}] + \frac{1}{T_1^0} \quad (1)$$

A smart agent to noninvasively map pH values with both high temporal and high spatial resolution would have broad utility. Decreased extracellular pH values are associated with cancer and ischemic diseases, such as stroke, ischemic heart disease, and kidney disease.[7] The pH of tissue could be a very useful biomarker for the identification of disease and monitoring of response to therapy, but it remains a challenge to routinely assess pH values in vivo. The implantation of a pH electrode is invasive and offers little spatial information. $^{31}$P NMR spectroscopy can be used to measure pH values on the basis of the pH-dependent chemical shift of inorganic phosphate.[8] The use of exogenous agents with pH-sensitive chemical shifts has also been described.[7,9] However, these NMR spectroscopic techniques are limited by low sensitivity, which results in trade-offs in imaging time (longer, more averages required) and resolution (lower, bigger-volume elements required). Chemical exchange saturation transfer (CEST) agents have also been described for pH imaging, but these agents are also required in millimolar concentrations for detection.[10,11] Recently, hyperpolarized $^{13}$C-carbonate MR was used to image pH values.[12]

There are several gadolinium-based smart agents whose relaxivity is pH-dependent owing to changes in complex hydration with changes in the pH.[6,7] To address the problem of complex concentration, Aime et al. proposed a $R_2/R_1$ ratiometric method,[13] where $R_2$ and $R_1$ are the transverse and longitudinal relaxation rates of water protons; however, given the relatively large inherent $R_2$ in living tissues relative to $R_1$, the in vivo accuracy of such an approach has yet to be proven. A combination of fluorine MRI for quantification with a pH-sensitive gadolinium-based agent has also been suggested,[14] although the sensitivity of $^{19}$F imaging is in the millimolar range.

An early pH-sensitive agent was GdDOTA-4AMP.[15] This agent was used to map pH values in vivo in renal-acidosis[16] and brain-tumor[17] models. To estimate the in vivo concentration of the agent, the investigators first injected GdDOTP, which shows pH-independent relaxivity, and imaged the regoin of interest. They assumed that the pharmacokinetics of GdDOTP was the same as for GdDOTA-4AMP, and that differences in the signal-versus-time curves for GdDOTP and GdDOTA-4AMP were due to differences in relaxivity. These studies demonstrated the potential for in vivo pH mapping and showed that MRI with GdDOTA-4AMP was sensitive enough to detect differences in pH. The limitations of this approach were the need for two sequential injections and the assumption that both contrast agents have identical pharmacokinetics.

Positron emission tomography (PET) offers exquisite sensitivity and the possibility of absolute quantification. Quantitative PET imaging is routinely used in human and animal studies, for example, to measure neuroreceptor occupancy levels[18] or to measure tissue perfusion.[19] The recent application of MR-compatible avalanche photodiode detector technology has now made it possible to have a

[*] Dr. L. Frullano, Dr. C. Catana, Dr. T. Benner, Prof. P. Caravan
A. A. Martinos Center for Biomedical Imaging
Massachusetts General Hospital, Harvard Medical School
149 13th Street, Suite 2301, Charlestown, MA 02129 (USA)
Fax: (+1) 617-726-7422
E-mail: caravan@nmr.mgh.harvard.edu
Prof. A. D. Sherry
Department of Chemistry, University of Texas at Dallas
and Advanced Imaging Research Center, Dallas (USA)

[**] This research was supported in part by the National Institute of Biomedical Imaging and Bioengineering, R21EB009738. MR–PET = magnetic resonance–positron emission tomography.

Supporting information for this article, including details of compound synthesis, relaxivity assays, and imaging experiments, is available on the WWW under http://dx.doi.org/10.1002/anie.201000075.


InterScience DISCOVER SOMETHING GREAT

© 2010 Wiley-VCH Verlag GmbH & Co. KGaA, Weinheim

functioning PET detector inside the MR magnet.[20,21] This setup enables the simultaneous acquisition of PET and MR data, and makes it possible to obtain both temporally and spatially registered imaging data sets. We hypothesized that simultaneous MR–PET imaging with a bimodal MR–PET smart agent would result in the quantification of both concentration and relaxivity. This dual-label approach could lead to a range of quantitative smart probes for in vivo applications.

Herein, we describe a bimodal MR–PET agent designed for quantitative pH imaging at concentrations commonly used for in vivo MRI (0.1–1 mM). The established pH-sensitive MR agent GdDOTA-4AMP was modified to incorporate a fluorine atom (either $^{18}F$ or $^{19}F$). Because of the hydrophilic character of highly charged GdDOTA-4AMP, the $^{18}F$ atom had to be introduced under aqueous conditions. We chose the versatile copper(I)-catalyzed Huisgen cycloaddition ("click reaction") for this purpose.[22] GdDOTA-4AMP-F was prepared in six steps in 19% overall yield from an established bifunctional chelator, *t*Bu-protected DOTAGA, **1** (Scheme 1).[23] Compound **1** was activated and coupled with propargylamine, and subsequently deprotected in neat trifluoroacetic acid (TFA) to give **3**. The phosphonate groups were introduced by coupling with aminomethylphosphonic acid diethyl ester, followed by mild deprotection of the phosphonate groups with trimethylsilyl bromide (TMSBr) in *N*,*N*-dimethylformamide (DMF). Finally, GdDOTA-4AMP-F was prepared from **5** in a one-pot process by treatment first with $GdCl_3$ to form the $Gd^{III}$ complex **6** and then with 2-fluoroethylazide. [$^{18}F$]Fluoroethylazide was prepared in two steps from 2-azidoethanol, whereas the isotopically unmodified compound was prepared in two steps from 2-fluoroethanol (see the Supporting Information).[22]

The introduction of the fluorine-containing moiety in GdDOTA-4AMP-F did not modify the pH dependence of the longitudinal relaxivity with respect to that of the parent compound GdDOTA-4AMP.[24] GdDOTA-4AMP-F retained

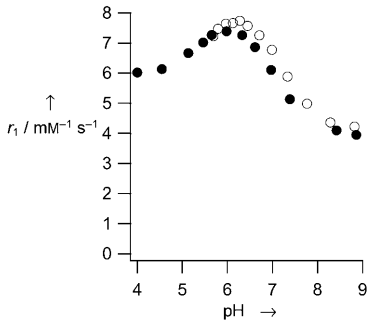


***Figure 1.*** Relaxivity of GdDOTA-4AMP-F as a function of pH value (37°C, 1.4 T) in the presence of NaCl (135 mM), KCl (5 mM), and $CaCl_2$ (2.5 mM; ●), and in rabbit plasma (○).

a monotonic decrease in relaxivity between pH 6.0 and 8.5 (Figure 1). In this pH range, the relaxivity varied between 7.4 and 3.9 mM$^{-1}$s$^{-1}$ (60 MHz, 37°C) when measured in an isotonic salt mixture. When the relaxivity was measured in rabbit plasma, the profile was found to be very similar to the profile measured in the salt solution. This result indicates little, if any, protein binding and suggests that the pH–relaxivity relationship will be valid in vivo.

The chemical concentration required for MR contrast is orders of magnitude higher than for PET imaging. For this reason, the $^{19}F$ and $^{18}F$ versions of the probe were prepared separately and subsequently mixed to produce a low-specific-activity MR–PET agent. Simultaneous MR–PET imaging was performed on a series of samples with varying pH values by using a clinical 3T magnetic resonance imager with an MR-compatible human PET scanner insert.[21]

Images were acquired by simultaneous MR–PET on two sets of phantoms: one in which $T_1$ was varied (MR, Figure 2A) and the probe concentration was constant (PET, Figure 2B), and one in which $T_1$ was constant (Figure 2C) and the probe concentration was varied (Figure 2D). Figure 2 eloquently displays the limitations of using an MR-responsive

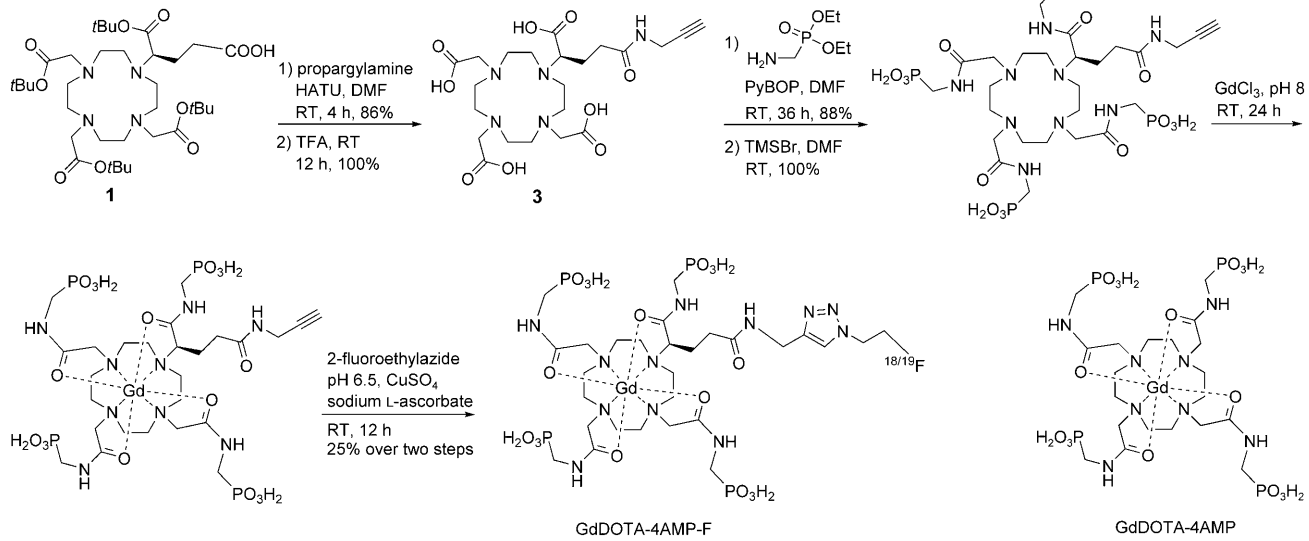


***Scheme 1.*** Synthesis of GdDOTA-4AMP-F and structure of GdDOTA-4AMP. Compounds **2** and **4** (not shown) can be found in the Supporting Information. HATU = *O*-(7-azabenzotriazol-1-yl)-*N*,*N*,*N*′,*N*′-tetramethyluronium hexafluorophosphate, PyBOP = benzotriazol-1-yloxytripyrrolidinophosphonium hexafluorophosphate.

 © 2010 Wiley-VCH Verlag GmbH & Co. KGaA, Weinheim 

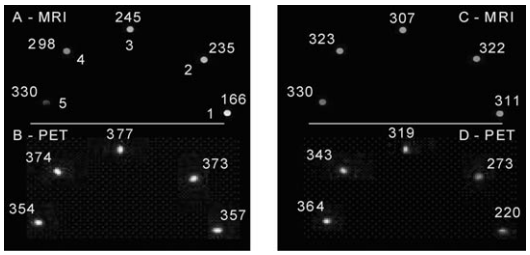


***Figure 2.*** A,C) $T_1$-weighted MR images (the $T_1$ values (ms) are given) and B,D) PET images (the PET intensities are given) of phantoms at pH 6.5 (tube 1), 6.8 (2), 7.1 (3), 7.4 (4), and 7.8 (5). Phantoms in images A and B had the same concentration (0.45 mM); phantoms in images C and D had the following concentrations: 0.31 (1), 0.33 (2), 0.38 (3), 0.42 (4), 0.45 mM (5).

agent without independent knowledge of the agent concentration. In both sets of phantoms, the pH value varied. The only way to obtain pH values from the images is to combine both PET and MR datasets.

Since the relationship between the PET signal and the radiochemical concentration is linear, the unknown agent concentration can be determined by comparing the PET images with a series of standards. For the MR data, the relationship between $r_1$ and the pH can be measured (see Figure 1); this process was repeated at 3T, and a similar linear relationship between $r_1$ and the pH was observed between pH 6 and 8.5. From these two standard curves, the PET and MR imaging data can be analyzed to estimate the pH of the samples. Figure 3 shows the good correspondence between the pH measured by a pH electrode and pH calculated from the MR and PET images.

In conclusion, we have described a smart MR–PET agent that can quantitatively and noninvasively report pH values. Imaging data were obtained on a commercial clinical MR imager with a prototype human PET camera at agent concentrations routinely encountered in clinical MRI (0.1–1 mM), which augurs well for the application of GdDOTA-4AMP-F to image pH changes in vivo. The combination of PET for the quantification of concentration and MR for the quantification of $T_1$ enables the simultaneous determination of relaxivity. With smart MR probes, whose relaxivity is proportional to an environmental stimulus, this bimodal imaging approach enables direct quantification of the stimulus, in this case the pH value. This bimodal MR–PET strategy is generally applicable to other smart MR probes.

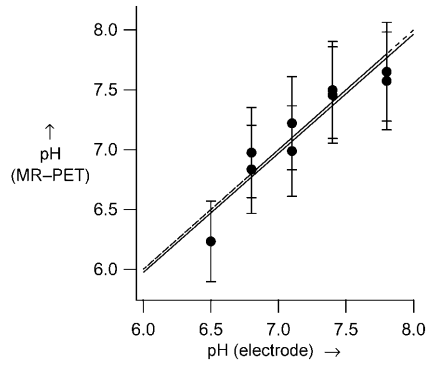


***Figure 3.*** Graph showing pH values obtained by analysis of the MR–PET images versus pH values measured with a glass electrode. The solid line is a linear fit of the data; the dotted line represents a 1:1 correspondence.

Received: January 6, 2010 [Z75]
Published online: February 28, 2010

**Keywords:** gadolinium · imaging agents · magnetic resonance imaging · pH imaging · positron emission tomography

[1] P. Caravan, *Acc. Chem. Res.* **2009**, *42*, 851.
[2] J. L. Major, T. J. Meade, *Acc. Chem. Res.* **2009**, *42*, 893.
[3] A. Y. Louie, M. M. Huber, E. T. Ahrens, U. Rothbacher, R. Moats, R. E. Jacobs, S. E. Fraser, T. J. Meade, *Nat. Biotechnol.* **2000**, *18*, 321.
[4] R. A. Moats, S. E. Fraser, T. J. Meade, *Angew. Chem.* **1997**, *109*, 749; *Angew. Chem. Int. Ed. Engl.* **1997**, *36*, 726.
[5] C. S. Bonnet, É. Tóth, *AJNR Am. J. Neuroradiol.*, DOI: ajnr.A1753.
[6] L. M. De Leon-Rodriguez, A. J. Lubag, C. R. Malloy, G. V. Martinez, R. J. Gillies, A. D. Sherry, *Acc. Chem. Res.* **2009**, *42*, 948.
[7] E. Pérez-Mayoral, V. Negri, J. Soler-Padrós, S. Cerdán, P. Ballesteros, *Eur. J. Radiol.* **2008**, *67*, 453.
[8] D. B. Kintner, M. K. Anderson, J. H. Fitzpatrick, Jr., K. A. Sailor, D. D. Gilboe, *Neurochem. Res.* **2000**, *25*, 1385.
[9] A. M. Kenwright, I. Kuprov, E. De Luca, D. Parker, S. U. Pandya, P. K. Senanayake, D. G. Smith, *Chem. Commun.* **2008**, 2514.
[10] S. Aime, D. Delli Castelli, E. Terreno, *Angew. Chem.* **2002**, *114*, 4510; *Angew. Chem. Int. Ed.* **2002**, *41*, 4334.
[11] K. M. Ward, R. S. Balaban, *Magn. Reson. Med.* **2000**, *44*, 799.
[12] F. A. Gallagher, M. I. Kettunen, S. E. Day, D. E. Hu, J. H. Ardenkjaer-Larsen, R. Zandt, P. R. Jensen, M. Karlsson, K. Golman, M. H. Lerche, K. M. Brindle, *Nature* **2008**, *453*, 940.
[13] S. Aime, F. Fedeli, A. Sanino, E. Terreno, *J. Am. Chem. Soc.* **2006**, *128*, 11326.
[14] E. Gianolio, R. Napolitano, F. Fedeli, F. Arena, S. Aime, *Chem. Commun.* **2009**, 6044.
[15] S. Zhang, K. Wu, A. D. Sherry, *Angew. Chem.* **1999**, *111*, 3382; *Angew. Chem. Int. Ed.* **1999**, *38*, 3192.
[16] N. Raghunand, C. Howison, A. D. Sherry, S. Zhang, R. J. Gillies, *Magn. Reson. Med.* **2003**, *49*, 249.
[17] M. L. Garcia-Martin, G. V. Martinez, N. Raghunand, A. D. Sherry, S. Zhang, R. J. Gillies, *Magn. Reson. Med.* **2006**, *55*, 309.
[18] C. M. Lee, L. Farde, *Trends Pharmacol. Sci.* **2006**, *27*, 310.
[19] F. M. Bengel, T. Higuchi, M. S. Javadi, R. Lautamaki, *J. Am. Coll. Cardiol.* **2009**, *54*, 1.
[20] C. Catana, D. Procissi, Y. Wu, M. S. Judenhofer, J. Qi, B. J. Pichler, R. E. Jacobs, S. R. Cherry, *Proc. Natl. Acad. Sci. USA* **2008**, *105*, 3705.
[21] H.-P. W. Schlemmer, B. J. Pichler, M. Schmand, Z. Burbar, C. Michel, R. Ladebeck, K. Jattke, D. Townsend, C. Nahmias, P. K. Jacob, W.-D. Heiss, C. D. Claussen, *Radiology* **2008**, *248*, 1028.
[22] M. Glaser, E. Årstad, *Bioconjugate Chem.* **2007**, *18*, 989.
[23] K. P. Eisenwiener, P. Powell, H. R. Macke, *Bioorg. Med. Chem. Lett.* **2000**, *10*, 2133.
[24] F. K. Kálmán, M. Woods, P. Caravan, P. Jurek, M. Spiller, G. Tircsó, R. Király, E. Brücher, A. D. Sherry, *Inorg. Chem.* **2007**, *46*, 5260.

 © 2010 Wiley-VCH Verlag GmbH & Co. KGaA, Weinheim 